Int. J. Heat Mass Transfer. Vol. 31, No. 7, pp. 1399–1408, 1988
Printed in Great Britain

0017–9310/88 $3.00 + 0.00

Experiment and analysis of forced convective heat transport in a packed bed of spheres

K. J. RENKEN† and D. POULIKAKOS
Department of Mechanical Engineering, University of Illinois at Chicago, P.O. Box 4348, Chicago, IL 60680, U.S.A.

(*Received* 27 *July* 1987 *and in final form* 13 *November* 1987)

Abstract—This paper presents an experimental investigation of forced convective heat transport in a packed bed of spheres occupying a heated channel. A parallel plate channel configuration with the channel walls maintained at constant temperature is employed. The experiments document the dependence of the temperature field as well as the heat flux from the wall (represented by the Nusselt number) on the problem parameters, in the thermally developing region. Numerical simulations for the same problem are also performed. A general model for the momentum equation accounting for flow inertia, macroscopic shear and variable porosity is used. The experimental and numerical findings are in good agreement and they predict an overall heat transfer enhancement between the wall and the fluid/porous matrix composite when compared to the predictions of the popular Darcy flow model.

1. INTRODUCTION

THE SUBJECT of convective heat transfer through a fluid-saturated porous medium represents a rapidly growing branch of thermal science. Several thermal engineering applications can benefit from a better understanding of convection through porous materials exemplified by geothermal systems, thermal insulations, grain storage, solid matrix heat exchangers, oil extraction, filtering devices and products manufactured in the chemical industry. The initial investigation of fluid flow through a porous medium originated in the nineteenth century with the engineering design of public fountains. Darcy [1] was the first to perform recorded experiments and to produce formulations pertaining to porous media. Since then the Darcy flow model has been employed by many engineering disciplines interested in the heat and flow characteristics of a porous matrix.

Although the Darcy flow model is popular in porous media convective heat transfer investigations because of its simplicity and good performance within the range of its validity, it neglects several physical effects of importance in channel flows. For example, by neglecting friction due to macroscopic shear the Darcy flow model does not satisfy the no-slip condition on a solid boundary. Next, the inertial forces which are significant for fast flows are disregarded. Finally, the spatial variation of the matrix porosity responsible for flow channeling near solid boundaries is ignored by the Darcy flow model. In the present experimental investigation the above effects are of importance. Therefore, a general flow model accounting for these effects will be tested against the experimental findings.

To this end, a theoretical investigation by Vafai and Tien [2] focused on the effects of a solid boundary and flow inertia on porous media boundary layer forced convection. These effects were shown to be more pronounced in highly permeable media, high Prandtl number fluids, large pressure gradients and in the region close to the leading edge of the boundary layer. The variable porosity effect has been investigated by several researchers [3–6] interested in velocity distributions in packed beds. Recent studies in refs. [7, 8] document experimentally and theoretically the effect of variable porosity in porous media flat plate forced convection. High porosity regions are found to exist in the vicinity of an impermeable boundary. The existence of high porosity close to an external boundary allows for channels of fast flowing fluid which significantly augment the heat transfer process in the system.

Although a considerable amount of theoretical work has been devoted to the principles of convection through porous media there exists a remarkable lack of published experimental results in all phases of the transport processes. Very few investigations have concentrated on forced convection which is a common heat transfer mode in porous media. Even fewer studies have compared modeling and experiments. An exception to this fact is the work of Vafai *et al.* [8] who reported an experimental and theoretical investigation on porous media flat plate boundary layer forced convection for a matrix consisting of packed spheres. Experimental results for the average Nusselt number are discussed. No local experimental heat transfer results were reported.

† Current address: Department of Mechanical Engineering, University of Wisconsin–Milwaukee, P.O. Box 784, Milwaukee, WI 53201, U.S.A.

NOMENCLATURE

A	Forchheimer's function, equation (8)
B	dimensionless pressure gradient, equations (12)
C_j	dimensionless coefficients, $j = 1, 2$, equations (12)
d	sphere diameter
d_*	dimensionless sphere diameter, d/H
D	channel height, Fig. 2
H	channel half height, Fig. 2
K	permeability, equation (7)
k_e	effective thermal conductivity of porous medium, equations (1) and (2)
Nu	Nusselt number, equation (3)
P	pressure
Pr	Prandtl number, ν/α_e
Q	flow rate
S	channel cross-sectional area
T	temperature
T_m	mixed mean temperature, $(\int \rho u T \, dS)/\rho VS$
u	horizontal velocity component
V	average velocity, $(\int u \, dS)/S$
x	horizontal Cartesian coordinate, Fig. 2
y	vertical Cartesian coordinate, Fig. 2.

Greek symbols

α_e	effective thermal diffusivity of porous medium
η	similarity variable, equation (13)
θ	dimensionless temperature, $(T_w - T)/(T_w - T_i)$
θ_m	invariant temperature, $(T_w - T)/(T_w - T_m)$
λ_j	constants, $j = 1, 2$, equation (9)
ν	kinematic viscosity
ρ	density
ϕ	porosity, equation (9).

Subscripts

i	channel inlet
w	channel wall
*	dimensionless quantity.

This paper presents an experimental study of forced convection in the thermally developing region of a channel packed with fluid-saturated spherical beads and bounded by two constant temperature parallel horizontal walls. The experimental setup measures the wall and the fluid/porous matrix composite temperatures and reports the local heat flux at the channel wall. Useful pressure measurements for various flow rates within the packed bed of spheres are also reported. The experimental findings are used to test a theoretical model for the same problem proposed by previous investigators [2, 8] and used by the present authors in an earlier study [9]. This model accounts for Forchheimer inertia, Brinkman friction and variable porosity. The experiments are performed in the regime of parameters where all the above effects are important [9]. In addition to the light the present study sheds on the fundamentals of convective heat transport in porous materials, it shows that porous matrices may constitute an attractive alternative for heat transfer augmentation in channels.

2. EXPERIMENTAL APPARATUS AND PROCEDURES

The apparatus employed in this study is shown schematically in Fig. 1. The setup is designed to provide accurate flow and temperature measurements. The objective of the experiment is to obtain the heat transfer parameters of interest for a parallel plate channel with constant temperature at the walls, packed with glass spheres.

The experimental apparatus is constructed of acrylic and aluminum both of which are 1.91 cm thick. The entrance section which is constructed entirely of acrylic has dimensions of $7.62 \times 15.2 \times 91.4$ cm (height $\times$ width $\times$ length) while the heated test section which contained only acrylic side walls has dimensions of $7.62 \times 15.2 \times 152$ cm. The parallel plate channel is packed with uniform 3 mm diameter soda lime glass spheres. Special care was taken in packing the beads to ensure uniformity in the structure of the porous medium. The spheres were poured randomly into the channel, levelled and then shook. After allowing the glass spheres to settle, more of the porous medium was placed in the channel and packed by the weight of the top plate. This procedure was repeated until no more glass spheres could be placed into the channel. Two stainless steel screens are placed at the inlet and outlet of the test section to hold the glass spheres in place. Two pressure taps are inserted from the channel side walls into the bed of packed spheres. A mercury U-tube manometer is used to measure experimentally the differential pressure within the porous medium channel. The precision of the manometer is dependent upon the liquid used and is approximately 12.4 Pa for mercury filled manometers. The accuracy is 1% full scale.

The top and bottom surfaces used to construct the heated parallel plates are 7750 alloy aluminum sheets. Both portions of the test section were removable so that the porous medium could be packed easily into the channel. The plate dimensions are $1.91 \times 19.0 \times 152$ cm. Ten mica strip heaters are clamped along the length of each aluminum plate 5.08 cm

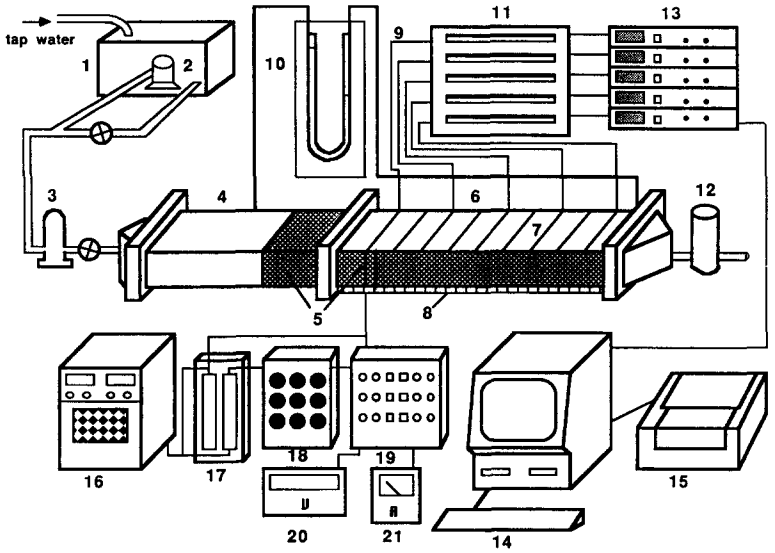

FIG. 1. 1, Water tank; 2, submersible pump; 3, water filter; 4, entrance section; 5, fluid saturated packed sphere bed; 6, heated section; 7, strip heaters; 8, insulation; 9, thermocouples; 10, U-tube mercury manometer; 11, thermocouple board; 12, rotameter; 13, data acquisition units; 14, personal computer; 15, printer; 16, power supplies; 17, copper strip board; 18, rheostat board; 19, circuit board; 20, voltmeter; 21, ammeter.

apart. Each strip heater could provide 500 W and a maximum sheath temperature of 900°F. For efficient operation, a thin layer of silicone heat sink compound was applied to the bottom of each heater which was then fastened firmly to the aluminum plates by 6.35 cm wide clamping bars. The entire heated test section was insulated with high temperature board. The 2.54 cm thick insulation could withstand the high temperature of the strip heaters and provide high thermal resistance. The estimated heat loss through the insulation was less than 2%. This loss is low indeed. The reasons for this fact are given below.

(a) The insulation board is especially designed for high temperature applications, i.e. the thermal conductivity of the board is very low.

(b) The plate temperatures were not very high. They varied between 10 and 40°C. The inlet water temperatures varied between 6 and 10°C.

(c) The strip heaters are manufactured so that the heating elements (the resistors inside the heaters) were located at the bottom of each heater which was in contact with the plate. A strip of insulation was placed on top of the resistors by the manufacturer, so that the top side of the heaters would remain relatively cool.

Two d.c. power supplies are used to power the strip heaters. By choosing to use d.c. power supplies we avoid fluctuations in the current that are associated with a.c. power supplies. As a result constant current through the strip heaters provides a constant plate temperature. Front panel monitoring of the power supplies allowed numerous current, voltage and power combinations to be employed. A copper strip board is used to place the 20 strip heaters in parallel. The heaters are then wired electrically to individual rheostats. These rheostats are high temperature, ceramic, variable resistors which can shunt large values of current. By decreasing or increasing the resistance of the rheostats, the temperature in each strip heater can be controlled. A circuit board is connected between the rheostats and the strip heaters to measure and monitor the current and the voltage in each strip heater without opening the circuit. An ammeter and a logging multimeter are used to measure current and voltage, respectively.

The temperature is monitored and recorded in the aluminum plates and throughout the porous medium by 148 copper–constantan thermocouples. A specific method of thermocouple fabrication was performed. The bare thermocouple wares were placed into a plier holder, twisted together and inserted into a thermocouple welding unit. An electrical arc and a purge of argon gas fused the dissimilar wires together to form a thermojunction. Argon gas was purged into the unit before, during and after welding to keep the environment clean. The thermojunction ball was approximately 0.5 mm in diameter. Each thermocouple was calibrated using an ice bath and found to be within ± 0.15°C. Thirty-two thermocouples (16 in each plate) were used to measure and monitor constant plate temperature. These thermocouples were threaded through a thermocouple brass sleeve and inserted into drilled wells on the two plates. The sleeves were firmly held by the strip heater clamping bars. The thermojunction ball remained at the tip of the sleeve and at the bottom of the well when inserted. One hundred and sixteen thermocouples were used to measure and record the temperature within the porous medium. Eleven thermocouple stations positioned

along the channel consisted of 10–14 thermocouples which were threaded and copper-oxidized into specially designed thermocouple nylon screen holders. The thermocouples nearest to the heated walls were placed at a distance 1.5 mm from these walls, so that measurements of the temperature within the thermal boundary layers were obtained. The holders were attached to framed screens which were inserted into machined grooves along the acrylic walls. The framed screens which had a porosity greater than the bed of packed spheres did not interfere with the flow in the channel.

A data acquisition system is used to measure accurately and swiftly the temperatures from the many thermocouples that were embedded in the porous medium and positioned in the plates. Five HP 3421A data acquisition/control units with 15 multiplexer assemblies were employed. The units contained thermocouple compensation and built-in Type T thermocouple linearization. A HP II personal computer along with a dual disc drive were used to monitor and record all the experimental temperature data onto microfloppy discs. A Basic program was formulated to monitor and collect wall and porous medium temperatures. Once the data were recorded onto the discs, various heat transfer parameters were calculated and printed.

Upstream of the test section was a water reservoir which stored the degassed tap water. To ensure particle free water, a water filter and a 5 μm polypropylene cartridge was inserted into the flow system at the entrance of the channel. Three air relief valves located in the entrance section of the channel allowed the removal of any air bubbles that may have passed through the water filter. A submersible pump and two globe valves controlled the flow rate range in the channel. The experimental setup permitted steady state flow conditions to be reached within a relatively short period of time. Flow rates were measured with an Omega, Inc. (Stamford, Connecticut) industrial rotameter. The range of flow rate was 0.757–9.46 l min^{-1} with a factory calibrated accuracy of $\pm 2\%$ full scale. An additional experimental check on the flow rate calibration produced negligible variation in measured values.

The procedure to collect experimental data was repeated rigorously for each test run. After a hydrodynamic steady state condition (constant Q) was reached, the power to the heaters was turned on. The total current, total voltage, and current and voltage for each strip heater were monitored by the front panels of the power supplies, the voltmeter and the ammeter. Close observations and recordings were made of the values of d.c. current which dictated the temperature of each strip heater. A constant plate temperature was reached by adjusting the rheostat resistances. The wall and the porous medium temperatures were monitored to determine when thermal steady-state conditions existed. When the thermocouple readings became constant, the Basic data acquisition program was run to collect and to store the experimental data. After each test run the channel was emptied, flushed and filled with water.

All of the fluid properties (density, specific heat, dynamic viscosity and thermal conductivity) were based on an average inlet temperature and calculated using regression curve fits. The standard error of the fluid property estimates was negligible. The experimental effective thermal conductivity was computed from empirical formulas supplied by the literature [10, 11]. The least complex of these are the parallel and series models while the Veinberg [12] model is applicable for all randomly packed spherical beds. The equations for the parallel and the Veinberg models which were used in the experimental calculations are, respectively

$$k_e = \phi_\infty k_f + (1-\phi_\infty)k_b \tag{1}$$

$$k_e + \phi_\infty \left[\frac{k_b - k_f}{k_f^{1/3}}\right] k_e^{1/3} - k_b = 0 \tag{2}$$

where ϕ_∞ is the experimental value of porosity at the core, k_f the thermal conductivity of the fluid and k_b the thermal conductivity of the soda lime glass spheres. Since the experimental value of k_e differed by less than 1% for the two models, an average value was used. The pressure gradient was determined by measuring the differential manometer height and the horizontal differential length. The velocity field with the porous medium channel had to be evaluated to determine the mixed mean temperature. Since no mechanical, electrical or other means are available to measure accurately a velocity profile within a fluid/porous matrix composite, an average velocity (slug profile) based on flow rate and porosity was calculated. To this end, it is felt that experimental techniques need to be developed in the future to accurately measure local fluid velocities in porous matrices. The mixed mean temperature, T_m, was evaluated by measuring the temperatures across the channel height and by employing a third-order polynomial integration formula. The wall temperature, T_w, was computed by averaging the 32 thermocouples that were embedded within the aluminum plates. The wall temperature of both plates was found to be uniform (within 0.5°C) for all experimental runs.

The experimental Nusselt number was determined as follows :

$$Nu = \left(\frac{\partial T}{\partial y}\right)_{y=0} \frac{D}{T_w - T_m} \tag{3}$$

where D is the channel height. The mixed mean temperature, T_m, was calculated as described above. The local temperature gradient, $(\partial T/\partial y)_{y=0}$, was evaluated by using the plate temperature and the reading of the thermocouple in the porous medium nearest to the wall, at each station. To check the validity of the temperature gradient calculation, the heat transfer rate from the wall to the fluid was also evaluated by measuring the current and the voltage and, next,

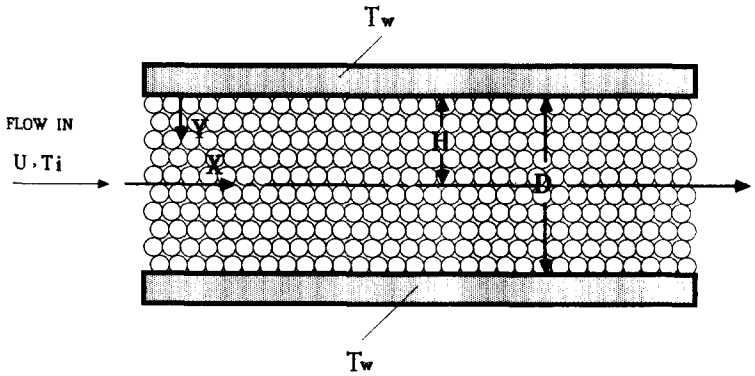

FIG. 2. Schematic for the numerical solution: parallel plate channel packed with a fluid-saturated bed of spheres.

determining the heat flux (power) produced by the strip heaters at the wall. Good agreement between the two methods was found.

3. NUMERICAL SIMULATIONS

Figure 2 shows a schematic of the system used for the numerical simulations, namely, the parallel plate channel filled with a fluid-saturated packed bed of spheres and bounded by two horizontal walls at constant temperature, T_w. The fluid at the channel inlet is isothermal at temperature, T_i ($T_i \neq T_w$). A fully developed velocity profile is assumed at the channel inlet. The coordinate system is also defined in Fig. 2.

Only the salient features of the numerical procedure will be described here. All the details are included in refs. [9, 13]. The velocity and temperature fields are described by the following momentum and energy equations and boundary conditions in which: (a) the macroscopic shear, the flow inertia and the variable porosity effects have been accounted for; (b) the buoyancy term has been neglected since the experimental and numerical studies deal only with forced convection; (c) the fluid and the porous medium are assumed to be in local thermal equilibrium and (d) the effective thermal diffusivity is constant. Neglecting the variation of thermal diffusivity while allowing for the porosity to vary in the numerical simulations is justified as follows. First, the analysis is simplified considerably. Without this approximation the numerical solution would be prohibitively cumbersome. Second, this approximation has been used very often by investigators of variable porosity problems [7, 8] with good results. Third, for the present problem, since the thermal conductivity of water is very close to the thermal conductivity of glass beads, neglecting the variation of α_e works well. It is true, however, that if the thermal conductivities of the porous matrix and the fluid are very different (such as in the case of copper and water) not accounting for the variation of α_e could yield a significant error

$$0 = -\frac{1}{\rho}\frac{dP}{dx} + \nu\frac{d^2u}{dy^2} - \frac{\nu}{K(y)}u - A(y)u^2 \qquad (4)$$

$$u\frac{\partial T}{\partial x} = \alpha_e\frac{\partial^2 T}{\partial y^2} \qquad (5)$$

$$u(0) = 0, \quad \left.\frac{\partial u}{\partial y}\right|_{y=H} = 0$$

$$T(x,0) = T_w, \quad \left.\frac{\partial T}{\partial y}\right|_{y=H} = 0. \qquad (6)$$

For a liquid-saturated porous medium the permeability, $K(y)$, and the flow inertia parameter, $A(y)$, depend on the matrix porosity and the sphere diameter as follows [14]:

$$K(y) = \frac{d^2\phi_3}{175(1-\phi)^2} \qquad (7)$$

$$A(y) = \frac{1.75(1-\phi)}{\phi^3 d}. \qquad (8)$$

The matrix porosity is assumed to be dependent on the distance from the impermeable wall. It has been shown [5, 7, 8] that for a bed of randomly packed spheres, the porosity decreases exponentially from the solid wall. The most commonly used equation for this exponential variation is [8]

$$\phi = \phi_\infty[1 + \lambda_1 e^{-\lambda_2 y/d}] \qquad (9)$$

where ϕ_∞ is the core porosity, d the sphere diameter and λ_1 and λ_2 empirical constants depending on the sphere diameter. Reliable experimental values for these constants in the porosity equation (9) are found in the literature [5] for the bead size employed in these forced convection experiments.

The above mathematical model, in which the heat and fluid flow characteristics are described, is solved by a numerical code employing a finite-difference scheme [9]. After non-dimensionalization, the governing equations (4) and (5) are transformed to

$$u_* + C_1(y_*)u_*^2 = BC_2(y_*) + C_2(y_*)\frac{\partial^2 u_*}{\partial y_*^2} \qquad (10)$$

$$u_* \frac{\partial \theta}{\partial x_*} = \frac{\partial^2 \theta}{\partial y_*^2} \tag{11}$$

where

$$x_* = \frac{x - x_i}{H\,Pr}, \qquad y_* = \frac{y}{H}$$

$$u_* = \frac{uH}{\nu}, \qquad \theta = \frac{T_w - T}{T_w - T_i}$$

$$C_1(y_*) = 10^{-2}\frac{d_*}{1-\phi}, \qquad C_2(y_*) = \frac{d_*^2 \phi^3}{175(1-\phi)^2}$$

$$B = -\frac{\partial P}{\partial x}\frac{H^3}{\rho \nu^2}. \tag{12}$$

To study the temperature field near the entrance of the heated region where the thermal boundary layer is very thin compared to the channel half height, H, the following similarity variable is introduced into the dimensionless energy equation (11) to achieve computational accuracy [15]:

$$\eta = \frac{y_*}{\sqrt{x_*}} \tag{13}$$

$$\frac{\partial^2 \theta}{\partial \eta^2} + u_* \frac{\eta}{2}\frac{\partial \theta}{\partial \eta} = u_* x_* \frac{\partial \theta}{\partial x_*} \tag{14}$$

$$\theta = 0 \text{ at } \eta = 0, \quad \theta = 1 \text{ at } \eta = \eta_{edge}. \tag{15}$$

Since the dimensionless momentum and energy equations are uncoupled, equation (10) can be solved independently to yield the velocity field. The temperature field can be obtained from equations (11) and (14). A variable grid in both the horizontal and vertical directions is used to produce accurate velocity and temperature results. The local heat flux at the channel wall is also evaluated numerically and cast into dimensionless form by means of the conduction referenced Nusselt number, equation (3). All the details of the numerical solution are reported in refs. [9, 13] and are not repeated here for brevity.

4. DISCUSSION OF RESULTS

In this section, the main results of the forced convection experiment are reported and compared with the numerical simulations. In obtaining the numerical results the following dimensionless input parameters were employed: the pressure gradient, the particle diameter, the empirical porosity constants and the Prandtl number. A constant value of effective thermal conductivity of the fluid-saturated porous medium is calculated from equations (1) and (2). The results are presented for the uniform 3 mm diameter soda lime glass spheres.

The dependence of the dimensionless pressure gradient, B, on the flow rate through the channel is reported in Fig. 3. It appears that when $B \sim 10^6$–10^7 the inertial effect (also known as the Forchheimer effect) is not negligible. A similar result was obtained in the numerical simulations of ref. [9]. Fand *et al.* [16] in a recent study reported measurements which aimed to define the various mechanisms, responsible for the pressure drop for flow in a packed bed of spheres. Their findings are in qualitative agreement with Fig. 3. The dimensionless temperature distribution across the channel half height is shown in Fig. 4 for two representative values of B and for the same distance from the channel inlet ($x = 7.62$ cm). Since the temperature measurements in Fig. 4 are for a station relatively close to the channel inlet, a sharp increase in the temperature is observed near the wall, after which the temperature in the channel remains constant, unaffected by the presence of the heated wall. Increasing the value of B (higher flow rate) yields a thinner thermal boundary-layer region. The agreement between experimentally and theoretically determined temperatures appears to be very good for both values of B.

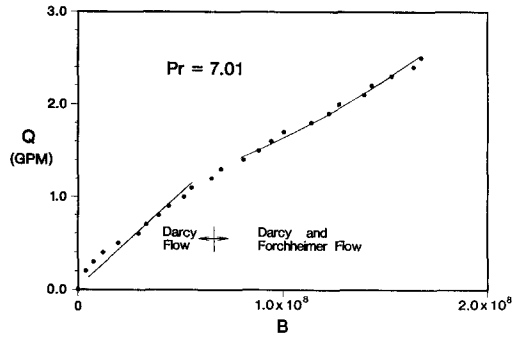

FIG. 3. Dependence of the dimensionless pressure gradient, B, on the flow rate, Q, through the packed bed of spheres.

Figure 5 illustrates temperature profiles for the same value of B and three different values of x. The heating effect of the wall is felt by a larger portion of the fluid/porous matrix composite at farther downstream positions. The agreement between experiment and theory is again good, better for smaller values of x. It appears that as we move downstream the theoretically obtained temperature field develops slower than the experimental temperature field. However, the theoretical model still predicts the temperature gradient at the wall quite well. Two reasons are suggested as to why the theoretical model lacks behind the real development of the temperature field. First, at these high values of dimensional pressure gradient, thermal dispersion [17] is probably important, enhancing thermal communication between the wall and the fluid/porous matrix composite. Thermal dispersion is neglected in the theoretical model. Second, the numerical simulations neglect the thermal diffusivity variation with porosity in the near wall region. It is speculated that if the above two effects (in particular the former) are accounted for in the

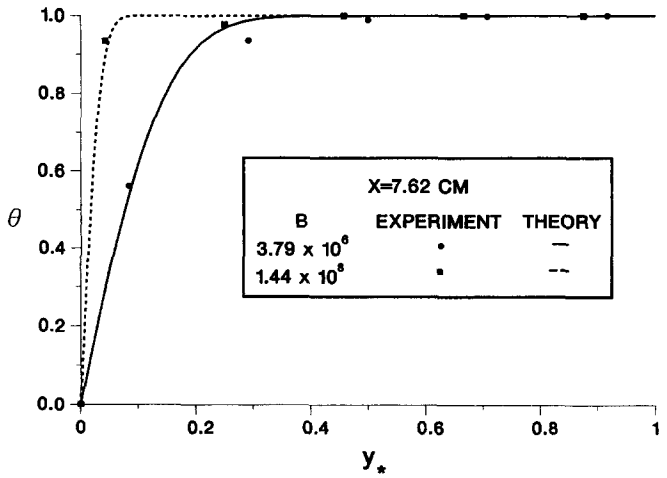

FIG. 4. Comparison of dimensionless temperature distribution across the channel half height for two values of parameter B.

theoretical modeling of forced convection in a channel, the agreement between theory and experiment will improve.

The effect of B on the invariant temperature profile is shown in Fig. 6. The agreement between theory and experiment is somewhat better for the larger value of B but overall it appears to be satisfactory. Invariant temperature profiles for the same value of B but different values of x are reported in Fig. 7. Much like for the dimensionless temperature profiles of Fig. 5, the theoretical model makes a better prediction of the physical situation near the channel entrance. Reasons for this circumstance were outlined in connection with Fig. 5.

Figure 8 presents the dependence of the thermal entry length, $x_{*\text{entry}}$, on the dimensionless pressure gradient represented by parameter B. The thermal entry length was determined as the distance between the channel entrance and the point at which the Nusselt number, Nu, and the invariant temperature, θ_m, become independent of the axial position. Experimentally, since the temperature measurements were taken at select downstream locations, it was estimated that the thermal entry length values were accurate within 10%. Only three points were obtained experimentally. A much longer (as much as five times longer) channel would be required to yield data points for the high range of B values used in the experiments. Increasing the value of B yields thinner thermal boundary layers on the two parallel plates which require a longer distance to produce a fully developed temperature field. The agreement between experiment and theory in Fig. 8 is good. The theoretical model overpredicts the experiment by approximately 25%. An additional point which is clear from the results in Fig. 8 is that the thermal entry length, is of significant extent, and the study of the thermal entry length problem in porous media channel flows is well justified.

Figures 9–11 report results for the Nusselt number in the thermal entry region. Both the experiment and

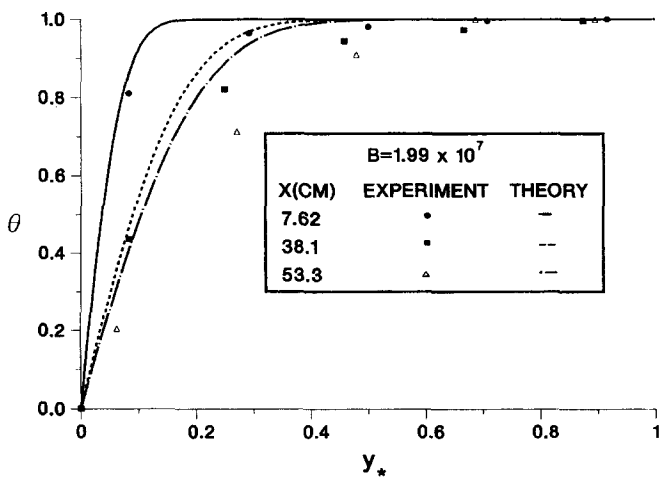

FIG. 5. Dimensionless temperature distributions across the channel half height for $B = 1.99 \times 10^7$ and for representative values of x.

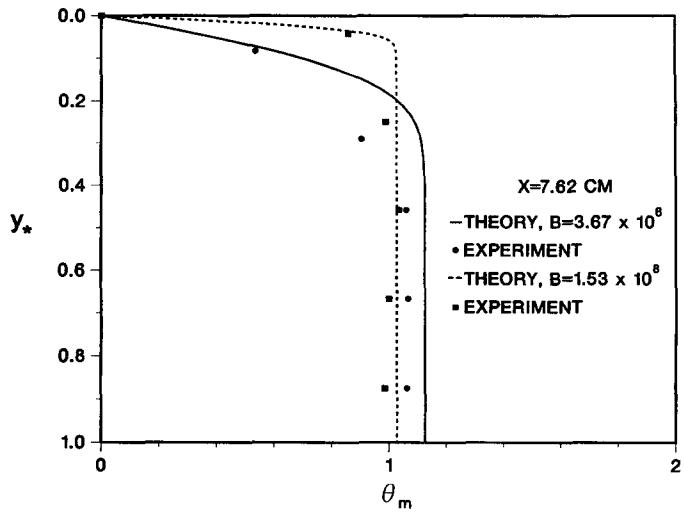

FIG. 6. The invariant temperature distribution across the channel half height for two values of parameter B.

the theoretical model are in good agreement and show that at downstream positions the value of Nu decreases until a plateau is reached corresponding to the fully developed region. In going from Fig. 9 to Fig. 11 (increasing B) the qualitative behavior is the same, however larger values of B yield thinner thermal boundary layers, hence, larger values of Nu in the thermal entry region. Keeping in mind that the measured and calculated values of Nu in all cases are consistently higher than the corresponding values for the same problem in classical fluids ($Nu = 3.77$ for parabolic flow) proves that the presence of the porous matrix enhances the heat transfer from the channel wall. Note that the Nusselt number results are also considerably higher than the classical fluids case of slug flow forced convection between two parallel plates ($Nu = 4.93$). The slug flow case coincides with the predictions of the Darcy flow model [9] in porous media (if the inertia, the macroscopic shear and the variable porosity effects are neglected in equation (4), the result is the Darcy flow model, $u \sim dP/dx \sim$ constant).

5. CONCLUSIONS

In this paper an experimental investigation of forced convection in a packed bed of spheres bounded by two isothermal walls is presented. Since experimental studies are scarce in the porous media heat transfer literature, the authors used their results to test an existing theoretical model accounting for the effects of macroscopic shear, flow inertia and variable porosity. The agreement between experiment and theory was good overall, better near the inlet of the

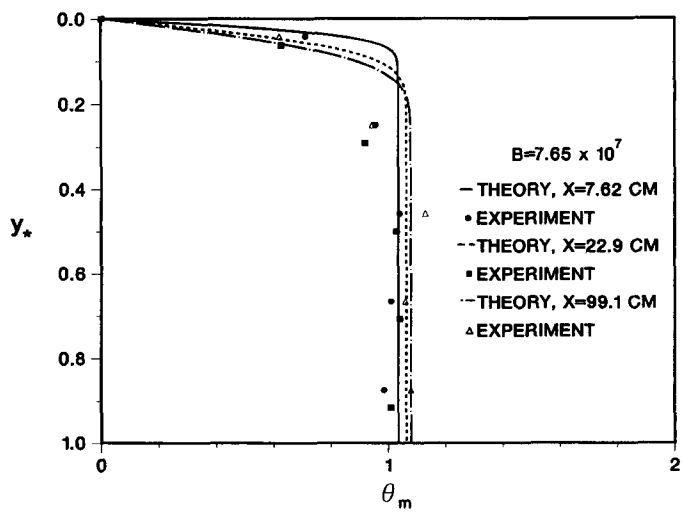

FIG. 7. The invariant temperature distribution across the channel half height for $B = 7.65 \times 10^7$ for representative values of x.

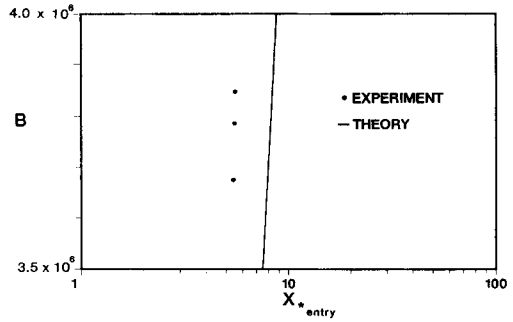

FIG. 8. Dependence of the thermal entry length on the dimensionless pressure gradient, B.

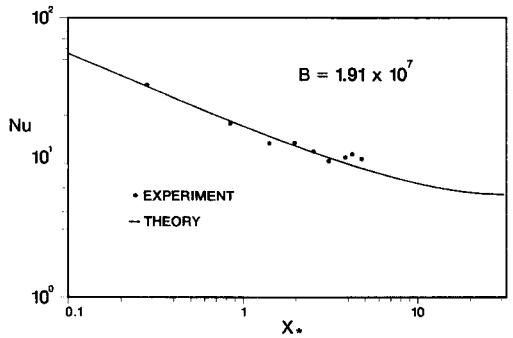

FIG. 9. Nusselt number variation with horizontal coordinate in the thermal entry region for $B = 1.91 \times 10^7$. The estimated overall error for the experimental values of Nu was 5.5%.

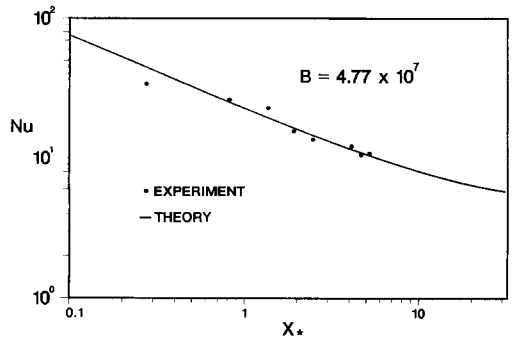

FIG. 10. Nusselt number variation with horizontal coordinate in the thermal entry region for $B = 4.77 \times 10^7$. The estimated overall error for the experimental values of Nu was 5.5%.

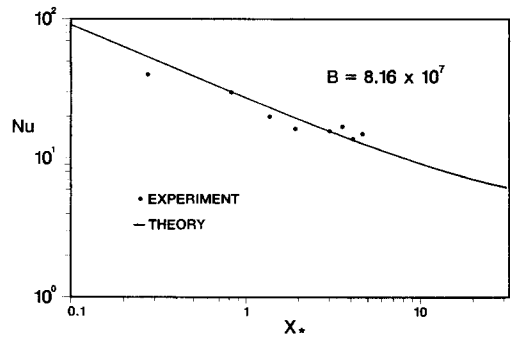

FIG. 11. Nusselt number variation with horizontal coordinate in the thermal entry region for $B = 8.16 \times 10^7$. The estimated overall error for the experimental values of Nu was 5.5%.

channel. The theoretical model predicted the temperature gradient at the wall throughout the channel length quite well. However, the theoretical temperature field developed slower than the experimental temperature field. It is speculated that effects such as thermal dispersion, if taken into account in future theoretical models, will improve the agreement between experiment and theory.

The length of the thermal entry region in the channel was significant and deserves the researcher's scrutiny. This is unlike the hydrodynamic entry length which was proven to be practically negligible in porous media flows. Increasing the dimensionless pressure gradient yielded sharper thermal boundary layers, enhanced heat transfer and resulted in a longer thermal entry region.

The Nusselt number measurements showed a significant increase in the local heat transfer at the channel wall relative to the results in classical fluids and to the predictions of the Darcy flow model in porous media. Based on this fact, the employment of porous media needs to be considered as a viable alternative for heat transfer augmentation in forced convection heat transport in channels.

Acknowledgement—Financial support for this research provided by the National Science Foundation through Grant ENG-8451144 and by the University of Illinois at Chicago Abraham Lincoln Graduate Fellowship is greatly appreciated.

REFERENCES

1. H. Darcy, *Les Fontaines Publiques de La Ville de Dijon*. Dalmont, Paris (1856).
2. K. Vafai and C. L. Tien, Boundary and inertia effects on flow and heat transfer in porous media, *Int. J. Heat Mass Transfer* **24**, 195–203 (1981).
3. C. E. Schwartz and J. M. Smith, Flow distribution in packed beds, *Ind. Engng Chem.* **45**, 1209–1218 (1958).
4. W. M. Schertz and K. B. Bischoff, Thermal and material transport in non-isothermal packed beds, *A.I.Ch.E. Jl* **15**, 597–604 (1969).
5. R. F. Benenati and C. B. Brosilow, Void fraction distribution in packed beds, *A.I.Ch.E. Jl* **8**, 359–361 (1962).
6. B. C. Chandrasekhara and D. Vortmeyer, Flow model for velocity distribution in fixed beds under isothermal conditions, *Thermo-Fluid Dynam.* **12**, 105–111 (1979).
7. K. Vafai, Convective flow and heat transfer in variable porosity media, *J. Fluid Mech.* **147**, 233–259 (1984).
8. K. Vafai, R. L. Alkire and C. L. Tien, An experimental investigation of heat transfer in variable porosity media, *J. Heat Transfer* **107**, 642–647 (1985).
9. D. Poulikakos and K. Renken, Forced convection in a channel filled with a porous medium including the effects of flow inertia, variable porosity and Brinkman friction, *J. Heat Transfer* **109**, 880–888 (1987).
10. J. A. Weaver and R. Viskanta, Freezing of liquid-saturated porous media, *J. Heat Transfer* **108**, 654–659 (1986).
11. M. A. Combarnous and S. A. Bories, Hydrothermal convection in saturated porous media. In *Advances in Hydroscience*, Vol. 10, pp. 231–307. Academic Press, New York (1975).
12. A. K. Veinberg, Permeability, electrical conductivity, dielectric conclusions, *Soviet Phys. Dokl.* **11**, 593–595 (1967).

13. K. J. Renken, Experiment and numerical modeling of forced convection heat transport in a channel filled with a porous medium, Ph.D. Thesis, University of Illinois at Chicago (1987).
14. W. Rohsenow and J. P. Hartnett (Editors), *Handbook of Heat Transfer*. McGraw-Hill, New York (1973).
15. T. Cebeci and P. Bradshaw, *Physical and Computational Aspects of Convective Heat Transfer*. Springer, New York (1984).
16. R. M. Fand, B. Y. K. Kim, A. C. C. Lam and R. T. Phan, Resistance to the flow of fluids through simple and complex porous media whose matrices are composed of randomly packed spheres, *J. Fluids Engng* **109**, 268–274 (1987).
17. J. T. Hong and C. L. Tien, Analysis of thermal dispersion effect on vertical-plate natural convection in porous media, *Int. J. Heat Mass Transfer* **30**, 143–150 (1987).

EXPERIENCE ET ANALYSE DU TRANSFERT DE CHALEUR PAR CONVECTION FORCEE DANS UN LIT FIXE DE SPHERES

Résumé—On présente une étude expérimentale de la convection forcée dans un lit fixe de sphères occupant un canal chauffé. On emploie un canal à plans parallèles maintenus à température constante. Les expériences précisent la dépendance du champ de température et du flux thermique pariétal (représenté par le nombre de Nusselt) sur les paramètres du problème dans la région de développement thermique. On réalise des simulations numériques du problème. On utilise un modèle général pour l'équation de quantité de mouvement prenant en compte l'inertie de l'écoulement, le cisaillement macroscopique et la porosité variable. Les résultats expérimentaux et numériques sont en bon accord et ils prédisent l'accroissement du transfert thermique global entre la paroi et le composite fluide/matrice poreuse en comparaison des prédictions du modèle classique de Darcy.

EXPERIMENTELLE UND THEORETISCHE UNTERSUCHUNG DES WÄRMETRANSPORTES BEI ERZWUNGENER KONVEKTION IN EINEM FESTBETT AUS KUGELIGEN PARTIKELN

Zusammenfassung—Es wird eine experimentelle Untersuchung des Wärmetransportes durch erzwungene Konvektion in einem Festbett aus kugeligen Partikeln, welches in einem beheizten Kanal untergebracht ist, berichtet. Der Kanal besitzt rechteckigen Querschnitt, seine Wände werden auf konstanter Temperatur gehalten. Für das thermische Einlaufgebiet wird die Abhängigkeit des Temperaturfeldes und der Wand-Wärmestromdichte (in Gestalt der Nusselt-Zahl) von den Versuchsparametern angegeben. Dasselbe Problem wird auch numerisch untersucht. Für die Impulstransport-Gleichung wird ein allgemeingültiges Modell verwendet, das Trägheitseffekte, makroskopische Schubspannungen und veränderliche Porosität enthält. Experiment und Theorie stimmen gut überein. Beide ergeben eine Verbesserung des Gesamt-Wärmeübergangs zwischen der Wand und dem System Fluid/poröse Matrix im Vergleich zu den Berechnungen nach dem bekannten Darcy'schen Strömungsmodell.

ЭКСПЕРИМЕНТАЛЬНОЕ И АНАЛИТИЧЕСКОЕ ИЗУЧЕНИЕ ВЫНУЖДЕННОГО КОНВЕКТИВНОГО ТЕПЛОПЕРЕНОСА В ПЛОТНОМ СЛОЕ, СОСТОЯЩЕМ ИЗ ШАРИКОВ

Аннотация—Представлено экспериментальное изучение вынужденного конвективного теплопереноса в плотном слое, состоящем из шариков, заполняющих плоскопараллельный нагретый канал, температура стенок которого поддерживается постоянной. Опыты подтверждают зависимость температурного поля и теплового потока от стенки (представленной числом Нуссельта) от параметров задачи в термически развивающейся области. Дано также численное решение задачи. Используется общая модель уравнения движения, учитывающая силы инерции потока, макроскопическое напряжение и меняющуюся порозность. Экспериментальные и численные данные хорошо согласуются между собой; они предсказывают интенсификацию теплообмена между стенкой и системой поток/пористая матрица по сравнению с известной моделью потока Дарси.